

KDM6B overexpression activates innate immune signaling and impairs hematopoiesis in mice

Yue Wei,¹ Hong Zheng,¹ Naran Bao,¹ Shan Jiang,² Carlos E. Bueso-Ramos,³ Joseph Khoury,³ Caleb Class,⁴ Yue Lu,⁵ Kevin Lin,⁵ Hui Yang,¹ Irene Ganan-Gomez,¹ Daniel T. Starczynowski,^{6,7} Kim-Anh Do,⁴ Simona Colla,¹ and Guillermo Garcia-Manero¹

¹Department of Leukemia, ²Institute for Applied Cancer Science, ³Department of Hematopathology, ⁴Department of Biostatistics, and ⁵Department of Epigenetic and Molecular Carcinogenesis, The University of Texas MD Anderson Cancer Center, Houston, TX; ⁶Division of Experimental Hematology and Cancer Biology, Cincinnati Children's Hospital Medical Center, Cincinnati, OH; and ⁷Department of Cancer Biology, University of Cincinnati, Cincinnati, OH

Key Points

- Overexpression of KDM6B mediates activation of innate immune signals and has a role in MDS and CMML pathogenesis.
- KDM6B targeting has therapeutic potential against MDS and CMML.

KDM6B is an epigenetic regulator that mediates transcriptional activation during differentiation, including in bone marrow (BM) hematopoietic stem and progenitor cells (HSPCs). Overexpression of KDM6B has been reported in BM HSPCs of patients with myelodysplastic syndromes (MDS) and chronic myelomonocytic leukemia (CMML). Whether the overexpression of KDM6B contributes to the pathogenesis of these diseases remains to be elucidated. To study this, we generated a Vav-KDM6B mouse model, which overexpresses KDM6B in the hematopoietic compartment. KDM6B overexpression alone led to mild hematopoietic phenotype, and chronic innate immune stimulation of Vav-KDM6B mice with the Toll-like receptor (TLR) ligand lipopolysaccharide (LPS) resulted in significant hematopoietic defects. These defects recapitulated features of MDS and CMML, including leukopenia, dysplasia, and compromised repopulating function of BM HSPCs. Transcriptome studies indicated that KDM6B overexpression alone could lead to activation of disease-relevant genes such as *S100a9* in BM HSPCs, and when combined with innate immune stimulation, KDM6B overexpression resulted in more profound overexpression of innate immune and disease-relevant genes, indicating that KDM6B was involved in the activation of innate immune signaling in BM HSPCs. Finally, pharmacologic inhibition of KDM6B with the small molecule inhibitor GSK-J4 ameliorated the ineffective hematopoiesis observed in Vav-KDM6B mice. This effect was also observed when GSK-J4 was applied to the primary BM HSPCs of patients with MDS by improving their repopulating function. These results indicate that overexpression of KDM6B mediates activation of innate immune signals and has a role in MDS and CMML pathogenesis, and that KDM6B targeting has therapeutic potential in these myeloid disorders.

Introduction

Myelodysplastic syndromes (MDS) and chronic myelomonocytic leukemia (CMML) are myeloid disorders originating from bone marrow (BM) hematopoietic stem and progenitor cells (HSPCs). Clinically, MDS and CMML are characterized by defective hematopoiesis, myeloid dysplasia, and a significantly increased risk of developing acute myelogenous leukemia.¹ Epigenetic and innate immune signals play critical roles in the regulation of BM HSPCs.² Consistently, molecular lesions affecting epigenetic and innate immune modulators are critical pathogenic mechanisms in MDS and CMML. The most important ones include somatic mutations of chromatin-modifying enzymes TET2, DNMTs, and EZH2³⁻⁸; overexpression of the innate immune signal activators Toll-like receptors (TLRs), TRAF6, IRAKs, Myd88, S100A8/A9, and mDia1⁹⁻¹⁴; and loss of the innate immune signaling brakes miR-146a, TIFAB, and RPS14.¹⁵⁻¹⁸

In agreement with these findings, studies from our laboratory have shown that KDM6B (JMJD3), an epigenetic modulator that positively regulates transcription of innate immune and developmental genes,^{2,19,20} is significantly overexpressed in BM HSPCs of patients with MDS and CMML.²¹ KDM6B is a JmjC domain histone demethylase that catalyzes the removal of the silencing methyl group on H3-Lys27 (H3K27).^{19,20} By interacting with the Set1/MLL methyltransferase, KDM6B also positively regulates the activating methylation of H3K4.² Our previous work provided evidence that, by modulating H3K4me3 and H3K27me3, KDM6B could activate transcription of several innate immune genes known to be overexpressed in MDS and CMML.²¹ By using primary patient BM HSPCs, we also demonstrated that KDM6B overexpression was associated with compromised hematopoietic differentiation.²¹ On the basis of these results, we hypothesize that KDM6B modulates and connects epigenetic and innate immune signals during hematopoiesis, and that overexpression of KDM6B has a role in MDS and CMML pathogenesis.

Patient specimens of MDS and CMML are highly heterogeneous, and there are few representative cell lines. Because of these limitations, most of the evidence regarding the contribution of KDM6B to MDS and CMML development is indirect, and therefore insufficient to define its pathogenic role. Hematopoiesis is also highly dependent on BM microenvironment. Therefore, we sought to study direct hematologic effects of KDM6B overexpression in a mouse model. Here we describe the generation studying of Vav-KDM6B mice and provide critical *in vivo* evidence that KDM6B overexpression promotes deregulation of innate immune signaling in hematopoietic disorders and is a pathogenic molecular aberration in MDS and CMML.

Materials and methods

Generation of transgenic mice

The cDNA of hCD4 was removed from HS21/25-Vav-hCD4 cells by BsiWI and NOT1. Human KDM6B cDNA was cloned from pDONR-221-hKDM6B (GeneCopaeia, Rockville, MD) and inserted into HS21/45-Vav vector. Cloning was performed by Epoch Life Science (Missouri City, TX). Cloning junctions were sequenced to verify. HS21/25-Vav-hKDM6B plasmid was digested with DrrI to remove a 1.8-kB backbone. The insert containing 5' and 3' Vav regulatory elements and hKDM6B cDNA was purified by gel electrophoresis. The construct was microinjected into zygotes obtained from C57BL/6 mice. Founders were identified by polymerase chain reaction (PCR), using primers that detected a common region between human and mouse KDM6B cDNA (GGAGACCTTTATCGCCTCTG/GGCAGCTTCTCCTCAGTGTT). Lines were maintained by mating wild-type (WT) C57BL/6 mice with founders. Offspring were genotyped by PCR of hKDM6B transgene from tail DNA. Mice were maintained in pathogen-free conditions. Animal care was in compliance with MD Anderson Cancer Center Institutional Care and Use Committee approval and US Department of Health and Human Services guidelines.

Characterization of mice

PB samples were collected in EDTA-coated tubes. Complete blood count analysis was performed using a HORIBA ABX Pentra analyzer. Animals were autopsied and BM and spleen tissues were examined. Tissue samples were fixed in 10% neutral-buffered

formalin (Fisher Scientific, Waltham MA), washed with phosphate-buffered saline (PBS), transferred into 70% ethanol, and stored at 4°C. Tissues were processed by the Research Histopathology Facility at MD Anderson Cancer Center.

Megakaryocyte morphology was evaluated on BM biopsy sections, as well as on Wright-Giemsa-stained aspirate smears. Dysmegakaryopoiesis was considered when megakaryocytes had the following features: micromegakaryocytes, megakaryocytes with nuclear hypolobation, and/or megakaryocytes with multinucleation.

Flow cytometry analysis

Single-cell suspensions of BM were incubated with antibodies and analyzed using a Gallios flow cytometer. Data were analyzed using the Kaluza flow cytometry analysis software. Lin[−]Sca1⁺cKit⁺ (LSK) was gated by Lin[−]Sca1⁺cKit⁺. We then used LSK/CD34[−]/Flt3[−] gating strategy for Figure 3A. When analysis of cell cycle or CD45.2 was needed in long-term hematopoietic stem cells (LT-HSC), we used the LSK/CD48^{low}/CD150^{high} LT-HSC gating in combination with other antibodies. These figures include Figure 3G and supplemental Figure 5A,G. Gating of other BM HSPCs includes that common myeloid progenitors were gated by Lin[−]Sca1[−]cKit⁺Flt3⁺CD34⁺; granulocyte-macrophage progenitors were gated by Lin[−]Sca1[−]cKit⁺Flt3[−]CD34⁺.

Methocult culture

Mouse LSK BM cells were added to Methocult3434 (StemCell Technologies, Vancouver, Canada) medium and plated at 300 cells per plate in 12-well culture dishes. Colonies were counted after 8 to 10 days.

BM engraftment

For noncompetitive transplantation, the CD45.2 old BM LSK cells were isolated and 10 000 LSKs were transplanted into each young and lethally irradiated CD45.1 recipient mouse, without support cells. For competitive transplantation, PB and BM chimerism after transplantation was assessed by fluorescence-activated cell sorting. Cells were stained with PE-CD45.1 and FITC-CD45.2 antibodies (BD Biosciences, San Jose, CA). Chimerism for each recipient was calculated on the basis of percentages of CD45.2⁺ and CD45.1⁺ cells.

LPS and GSK-J4 injection

Lipopolysaccharide (LPS; 6 μg/mouse) was injected into the peritoneal space of mice every other day for 6 weeks under sterile conditions.²¹ LPS was diluted in sterile PBS at a concentration of 30 μg/mL. GSK-J4 (8 mg/kg) was injected into the peritoneal space of mice once a week for 4 weeks under sterile conditions.²² GSK-J4 was diluted in sterile dimethyl sulfoxide-ethanol solution.

RNA-Seq

RNA from sorted BM LSK cells was isolated using the PicoPure RNA isolation kit (Fisher Scientific).

RNA-Seq sequencing libraries were made using the SMARTer v4+ Nextera kit. The libraries were sequenced using a 2 × 75 bases paired-end protocol on an Illumina HiSeq 3000 instrument, and 55 to 115 million pairs of reads were generated per sample. Each pair of reads represents a cDNA fragment from the library. The reads were mapped to the mouse genome (mm10) by TopHat (version 2.0.10). By reads, the overall mapping rate was 91% to 93%, and 86% to 88% of fragments had both ends mapped to the mouse genome. The number of fragments in each known gene from the

RefSeq database (downloaded from UCSC Genome Browser on 17 July 2015) was enumerated using htseq-count from the HTSeq software package (version 0.6.0). Genes with fewer than 10 fragments in all the samples were removed before differential expression analysis. The differential expression between conditions was statistically assessed by edgeR (version 3.8.6). Genes with a false discovery rate ≤ 0.05 , fold change ≥ 1.5 , and length > 200 bp were called as differentially expressed.²² Pathway enrichment analysis was performed using gene set enrichment analysis.

The overlap between differentially expressed genes in the mouse and human experiments was assessed using Fisher's exact test, including only the genes that have both mouse and human homologs. To correlate KDM6B expression with the signature in CMML, the log₂-expression of the 41 signature genes was averaged within each patient, and the Pearson correlation coefficient of this value vs KDM6B expression across patient samples was calculated.

Isolation and culture of human BM CD34⁺ cells

BM was obtained from patients via needle aspiration, and the diagnosis of MDS or CMML was confirmed by a hematopathologist. BM samples from healthy individuals were obtained from AllCells (Emeryville, CA). CD34⁺ cells were isolated using MicroBead Kit (Miltenyi Biotec). For colony formation, BM CD34⁺ cells were seeded at 3×10^3 cells/plate in 12-well culture dishes with GFH4434 medium (StemCell Technologies). Colonies were evaluated after 2 weeks of culture.

Statistical analysis

Data were analyzed by a Student *t* test, and $P < .05$ was considered to be statistically significant. $P < .01$ is considered as a strong tendency, and the results are reflected in the figures. For data displaying error bars, the standard error of the mean (SEM) was calculated to indicate the variation within data set.

Results

Generation of Vav-KDM6B mice

Vav-KDM6B mice overexpressing the human transgene KDM6B in hematopoietic cells were generated by cloning human KDM6B cDNA into HS21/45-Vav vector,^{23,24} followed by microinjection into C57BL6 mice. To make sure the phenotype in Vav-KDM6B mice was not a result of supraphysiological overexpression of the transgene, we evaluated KDM6B mRNA and selected 1 transgenic line that exhibited 10-fold KDM6B overexpression in BM (Figure 1A) in a manner similar to KDM6B overexpression in human MDS/CMML.²¹ Vav-KDM6B mice were born at expected Mendelian ratios and appeared physically normal. KDM6B is known to actively regulate production of inflammatory cytokines.^{2,25} We performed an enzyme-linked immunosorbent assay of peripheral blood (PB) serum and detected increases in KDM6B-regulated tumor necrosis factor and CXCL2 (MIP-2) in Vav-KDM6B mice (supplemental Figure 1A-B), indicating that the transgenic KDM6B was functional.

KDM6B overexpression resulted in moderately impaired hematopoiesis and BM dysplasia

We observed that Vav-KDM6B mice at 20 to 30 weeks of age exhibited a mild hematological phenotype, including a subtle but significant reduction of white blood cell counts (Figure 1B) affecting

mostly neutrophils (Figure 1B), slightly lower lymphocytes (supplemental Figure 1C), and a nonsignificant reduction of cell counts in BM compartment ($P < .1$; supplemental Figure 1D). Aged Vav-KDM6B mice had increased mortality compared with WT mice, starting at approximately 20 months of age (80 weeks; Figure 1C). Survival analysis (36 months) demonstrated that Vav-KDM6B mice ($N = 24$) had a median age of 28 months, whereas the median age in control WT mice ($N = 18$) was not reached by the end of our 36-month experiment ($P < .05$; Figure 1C).

We therefore analyzed whether overexpression of KDM6B led to severe hematological effects in aged mice. In the PB of aged Vav-KDM6B mice (70 weeks old), reduction of white blood cells compared with in WT mice was greater than in younger Vav-KDM6B mice (Figure 1D). A slight but significant reduction of red blood cells was also observed in aged Vav-KDM6B mice (supplemental Figure 1E). In the BM of aged Vav-KDM6B mice, we observed an increased frequency of dysplasia in megakaryocytes (Figure 1E). For BM HSPCs, although old Vav-KDM6B and age-matched WT mice exhibited similar frequencies of HSPCs (supplemental Figure 1F-K), the function of LSK (lineage⁻, cKit⁺, Sca1⁺) in aged Vav-KDM6B mice to form colonies was decreased compared with LSK of WT mice in first plating (G1; Figure 1F). These results became significant with the second plating (G2; Figure 1F). Hematopoietic marks in cells collected from methylcellulose had no significant differences between KDM6B and WT groups (supplemental Figure 1J-L). We further assessed the in vivo repopulating capacity of aged BM LSKs by transplanting them into lethally irradiated young recipients. Recipients reconstituted with Vav-KDM6B LSKs exhibited a steady pattern of reduced PB white blood cell counts (Figure 1G). At 12 months after transplantation, the BM of mice reconstituted with Vav-KDM6B cells exhibited significantly reduced frequencies of LSK (Figure 1H), Gr1⁺ myeloid (Figure 1I), and B220⁺ lymphoid cells (supplemental Figure 1M). These results indicate that overexpression of KDM6B leads to progressively impaired repopulating function in BM HSPC with aging. Importantly, the phenotypes of Vav-KDM6B mice, including PB leukopenia, BM dysplasia, and impaired repopulating capacity of BM HSPCs, are reminiscent of key pathologic features observed in low-risk patients with MDS.

Chronic innate immune stimulation led to significant leukopenia and dysplasia in Vav-KDM6B mice

Chronic inflammation and innate immune signaling play a role in the pathogenesis of MDS.⁴ Moreover, the BM microenvironment of patients with MDS and aged mice have increased levels of TLR ligands, such as S100A8/A9,¹² suggesting that TLR stimulation may accelerate the hematopoietic defects observed in MDS. To determine whether KDM6B overexpression cooperated with TLR-mediated innate immune activation in MDS pathogenesis, we studied the effects of chronic low-dose TLR ligand LPS stimulation (6 μ g/mouse, every other day for 6 weeks) in Vav-KDM6B mice. This low-dose LPS regimen has been demonstrated to be safe and cause minor hematopoietic alterations in WT mice,²⁶ and led to no significant changes in KDM6B mRNA expression in BM (supplemental Figure 2A). Compared with LPS-treated WT mice, Vav-KDM6B mice treated by LPS had significantly reduced PB white blood cell, neutrophil, and lymphocyte counts (Figure 2A-B; supplemental Figure 2B) and slightly reduced platelets (supplemental Figure 2C). In the BM compartment, LPS-treated

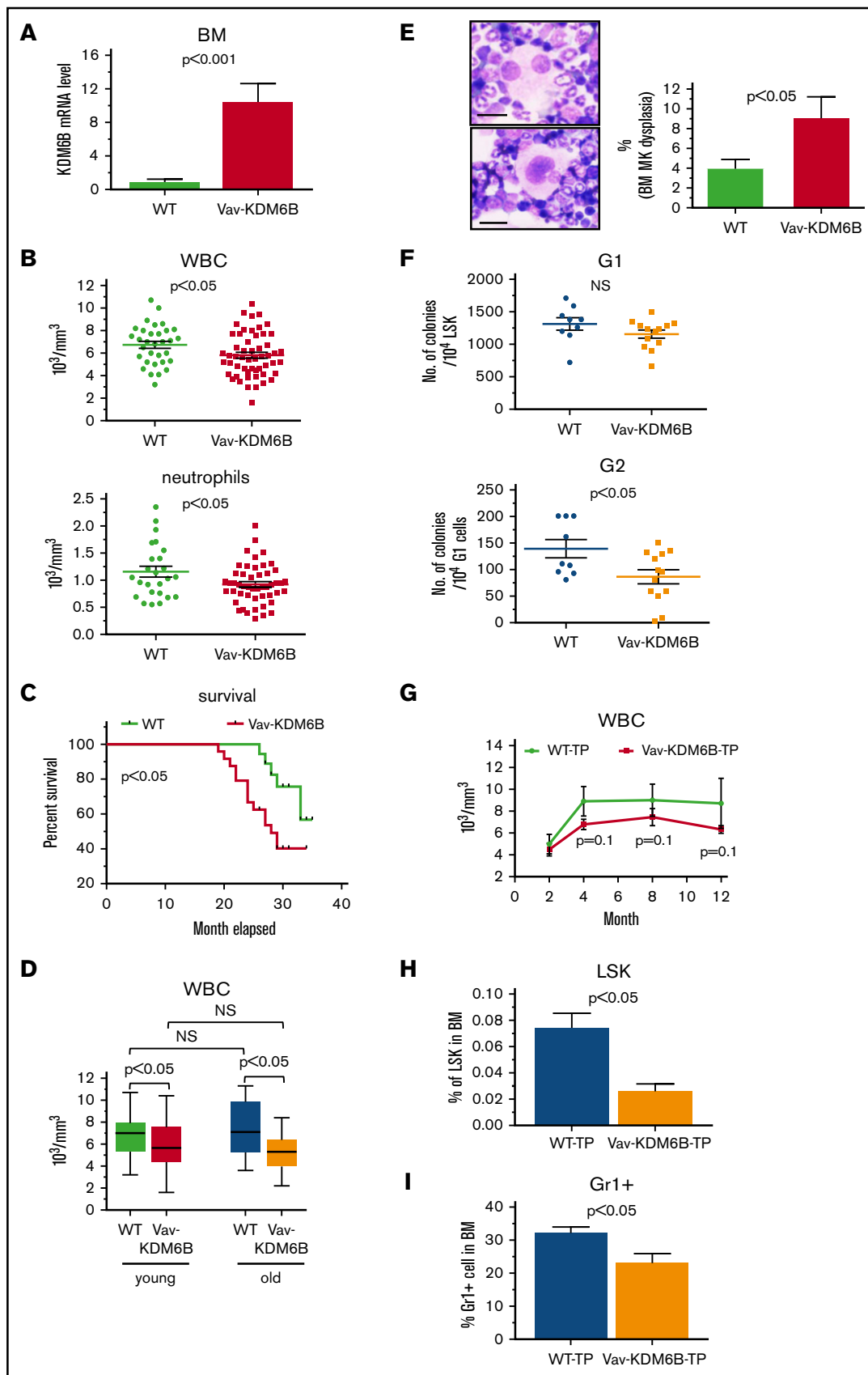


Figure 1.

Vav-KDM6B mice had a greater reduction in BM counts (Figure 2C-D), as well as Gr1⁺ myeloid and B220⁺ lymphoid populations (Figures 2E-F). Reduced red blood cells and erythroid markers (CD71) were observed in the BM of both LPS-treated WT and Vav-KDM6B mice (supplemental Figure 2D-E), but the effect was slightly stronger in the red blood cells of Vav-KDM6B mice. Furthermore, increased dysplasia in BM megakaryocytes was detected in LPS-treated Vav-KDM6B mice (Figure 2G-H). Collectively, these results demonstrate that chronic innate immune stimulation mediated by low-dose LPS leads to changes in Vav-KDM6B mice that mimic MDS.

KDM6B overexpression in combination with chronic innate immune stimulation results in altered BM HSPCs and compromised BM repopulating potential

We then examined whether the MDS/CMML-like phenotype observed in LPS-treated Vav-KDM6B mice was the result of impairment of BM HSPCs. LPS specifically led to a significantly reduced frequency of long-term hematopoietic stem cell population (LT-HSC, LSK/CD34⁺/Flt3⁺) in Vav-KDM6B mice (Figure 3A) compared with PBS-treated Vav-KDM6B mice. Gating of this population and representative fluorescence-activated cell sorting plots are shown in supplemental Figure 3. Similar observations were also made when the long-term population was analyzed by Lin⁺/cKit⁺/CD150^{high}/CD48^{low} or LSK/CD150^{high}/CD48^{low} (supplemental Figures 4 and 5A). We also performed Ki67 labeling in the Lin⁺/cKit⁺/CD150^{high}/CD48^{low} LT population, which revealed that LPS led to a decrease of cell cycle G0 phase in cells of both WT and Vav-KDM6B mice (supplemental Figure 5B), suggesting a loss of quiescence. In BM progenitors, treatment with LPS resulted in a significantly reduced frequency of common myeloid progenitors in Vav-KDM6B mice (Figure 3B; supplemental Figure 3) compared with PBS-treated Vav-KDM6B mice.

We then performed colony formation assays to analyze the repopulating function of BM HSPCs, using LSKs isolated from PBS or LPS-treated mice. Starting from the second plating (G2), the number of colonies formed by LSKs from Vav-KDM6B mice was significantly lower than that from WT mice (Figure 3C). Furthermore, although LPS treatment in WT and Vav-KDM6B mice led to reduced LSK-derived colonies (Figure 3C), the number of colonies formed by LSKs of LPS-treated Vav-KDM6B mice was the lowest among all experimental groups (Figure 3C). Although no significant difference in hematopoietic marks was observed in cells collected from methylcellulose (supplemental Figure 5C-E), these results suggest that KDM6B overexpression and LPS-mediated innate immune activation cooperatively suppress the repopulating function of BM HSPCs.

To further confirm this, we performed competitive BM transplantation assays. Mice were first treated with PBS or LPS for 6 weeks. Next, CD45.2 BM cells were isolated from treated mice and mixed with competitive WT CD45.1 BM cells and transplanted into lethally irradiated CD45.1 recipients. No innate immune stimulation was administered to recipients before or after transplantation. PB chimerism in the recipients was analyzed. As shown in Figure 3D-E, PB and PB-myeloid (Gr1⁺) chimerisms (CD45.2) in the recipients transplanted with BM cells of LPS-treated Vav-KDM6B mice were significantly lower and progressively declined compared with PBS-treated Vav-KDM6B or LPS-treated WT mice. Similar observations were also made for PB-lymphoid (B220⁺) cells (supplemental Figure 5F). Six months after transplantation, significantly lower BM chimerism (CD45.2) was detected in the recipients transplanted with BM cells of LPS-treated Vav-KDM6B mice compared with PBS-treated Vav-KDM6B (Figure 3F). In BM HSPCs, KDM6B overexpression in combination with LPS also resulted in lower CD45.2 chimerisms in LT-HSC (LSK/CD150^{high}/CD48^{low}; Figure 3G), common myeloid progenitor, and granulocyte-macrophage progenitor (supplemental Figure 5G-H) populations. Collectively, these findings indicate that KDM6B overexpression in combination with innate immune activation results in a significantly compromised repopulating function in BM HSPC.

KDM6B overexpression in combination with chronic innate immune stimulation resulted in activation of MDS-relevant innate immune genes in BM HSPCs

KDM6B regulates transcription via epigenetic dependent and independent mechanisms.^{2,27} Therefore, to dissect the molecular mechanisms underlying the MDS/CMML-like phenotype observed in Vav-KDM6B mice, we performed genome-wide RNA expression analyses.

Whole-exome RNA-Seq was first performed in donor-derived BM LSKs from the recipients transplanted with aged LSKs (described in Figure 1G-I). Eighteen genes were identified as significantly overexpressed (>1.5-fold; $P < .05$) in Vav-KDM6B LSKs compared with the WT counterpart (supplemental Figure 6A). To elucidate the mechanisms underlying the combinational effect between KDM6B overexpression and chronic LPS stimulation, we performed whole-exome RNA-Seq in BM LSKs collected from the mice after chronic LPS or PBS treatment (described in Figure 3A). LPS treatment resulted in a more profound transcription activation in LSKs of Vav-KDM6B mice than in WT counterparts (supplemental Figure 6C): 135 genes were significantly overexpressed after LPS treatment (>1.5-fold; $P < .05$) in LSKs of Vav-KDM6B mice as compared with that in WT mice (Figure 4A).

Figure 1. Overexpression of KDM6B in Vav-KDM6B mice led to moderately impaired hematopoiesis and bone marrow dysplasia. (A) Relative mRNA expression levels of human KDM6B in bone marrow (BM) cells of adult Vav-KDM6B (N = 16) and WT (N = 12) mice. (B) Complete blood count results for WBCs and neutrophils of adult Vav-KDM6B mice (N = 46) compared with littermate WT controls (N = 27). (C) Kaplan-Meier survival curves of Vav-KDM6B (N = 24) and WT (N = 18) mice. (D) WBC counts in old (age > 70 weeks) Vav-KDM6B mice (N = 19) and age-matched WT controls (N = 15) compared with young (age 20-30 weeks) mice. (E) Example images of BM cytopsin showing megakaryocytic dysplasia and in old Vav-KDM6B mice (N = 6) and age-matched WT controls (N = 4). Scale bars represent 15 μ m. (F) Primary (G1) and secondary (G2) plating colony-forming units in serial methylcellulose colony formation assays of lineage-negative, cKit-positive, Sca1-positive (LSK) BM cells isolated from old, age-matched WT (N = 9) and Vav-KDM6B (N = 13) mice. (G) Kinetics of peripheral blood WBC counts in recipient mice transplanted with LSK BM cells of old, age-matched WT (N = 4) and Vav-KDM6B (N = 7) mice. (H-I) Percentages of LSK BM cells and Gr1⁺ cells in recipient mice transplanted with LSK BM cells of old Vav-KDM6B (N = 7) and age-matched WT (N = 4) mice. All error bars are based on \pm SEM.

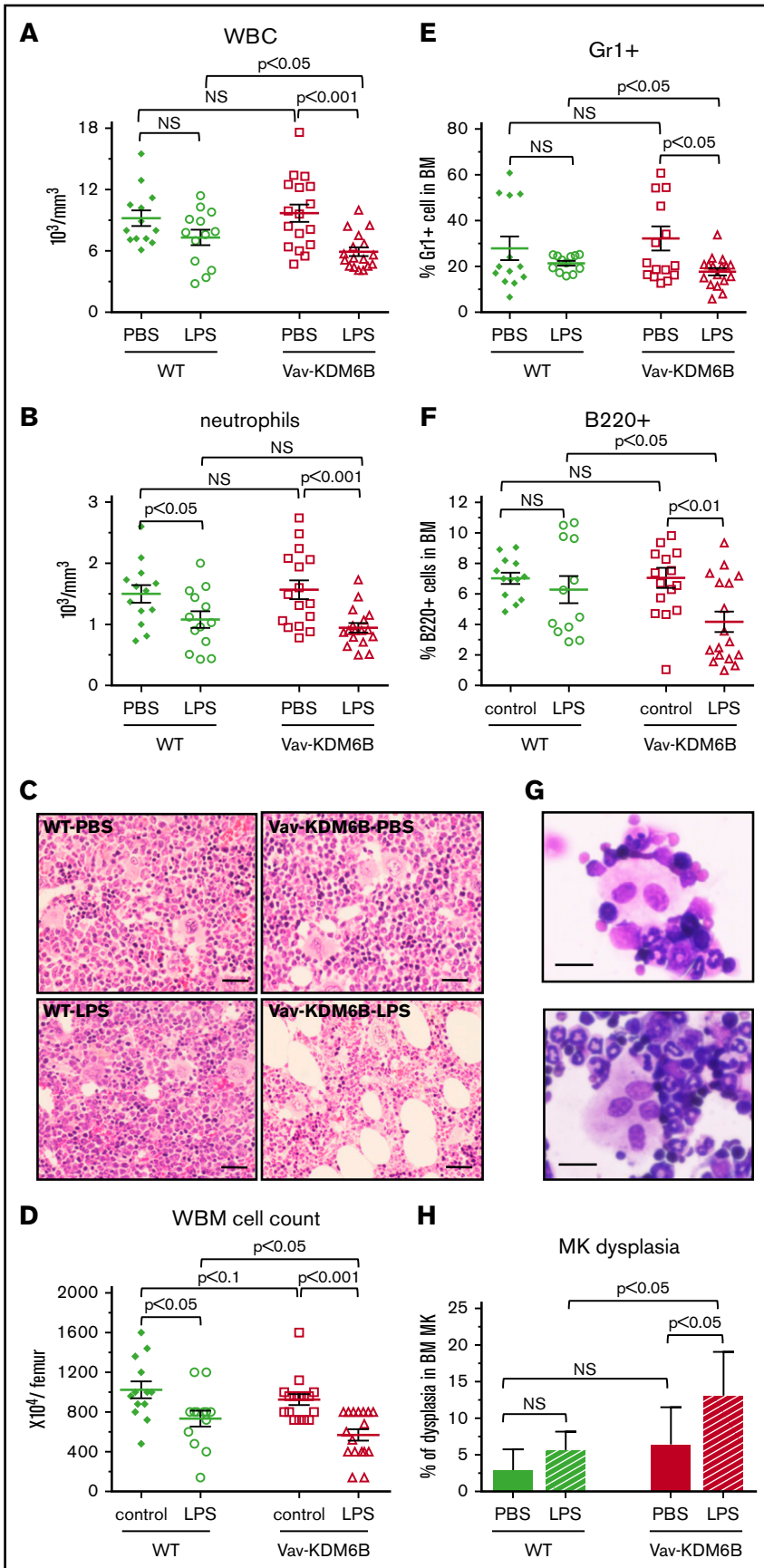


Figure 2. Chronic low-dose LPS stimulation of Vav-KDM6B mice led to a MDS-like hematopoietic phenotype. Results are based on adult Vav-KDM6B mice and WT controls treated with low-dose LPS (6 μ g/mouse) or PBS every other day for 6 weeks (LPS: N = 13 Vav-KDM6B, N = 13 WT; PBS: N = 17 Vav-KDM6B, N = 17 WT, unless otherwise noted). All error bars are based on \pm SEM. (A-B) Complete blood count results for WBCs and neutrophils. (C) Example images of hematoxylin and eosin-stained BM sections of indicated mice. Scale bars represent 1 mm. (D) Whole BM (WBM) cell counts. (E-F) Percentages of myeloid (Gr1-positive) and lymphoid (B220-positive) cells in the BM of indicated mice. (G-H) Example images and counts of BM cytopsin showing megakaryocytic dysplasia in LPS-treated KDM6B mice (LPS: N = 4 Vav-KDM6B, N = 4 WT; PBS: N = 5 Vav-KDM6B, N = 5 WT). Scale bars represent 15 μ m.

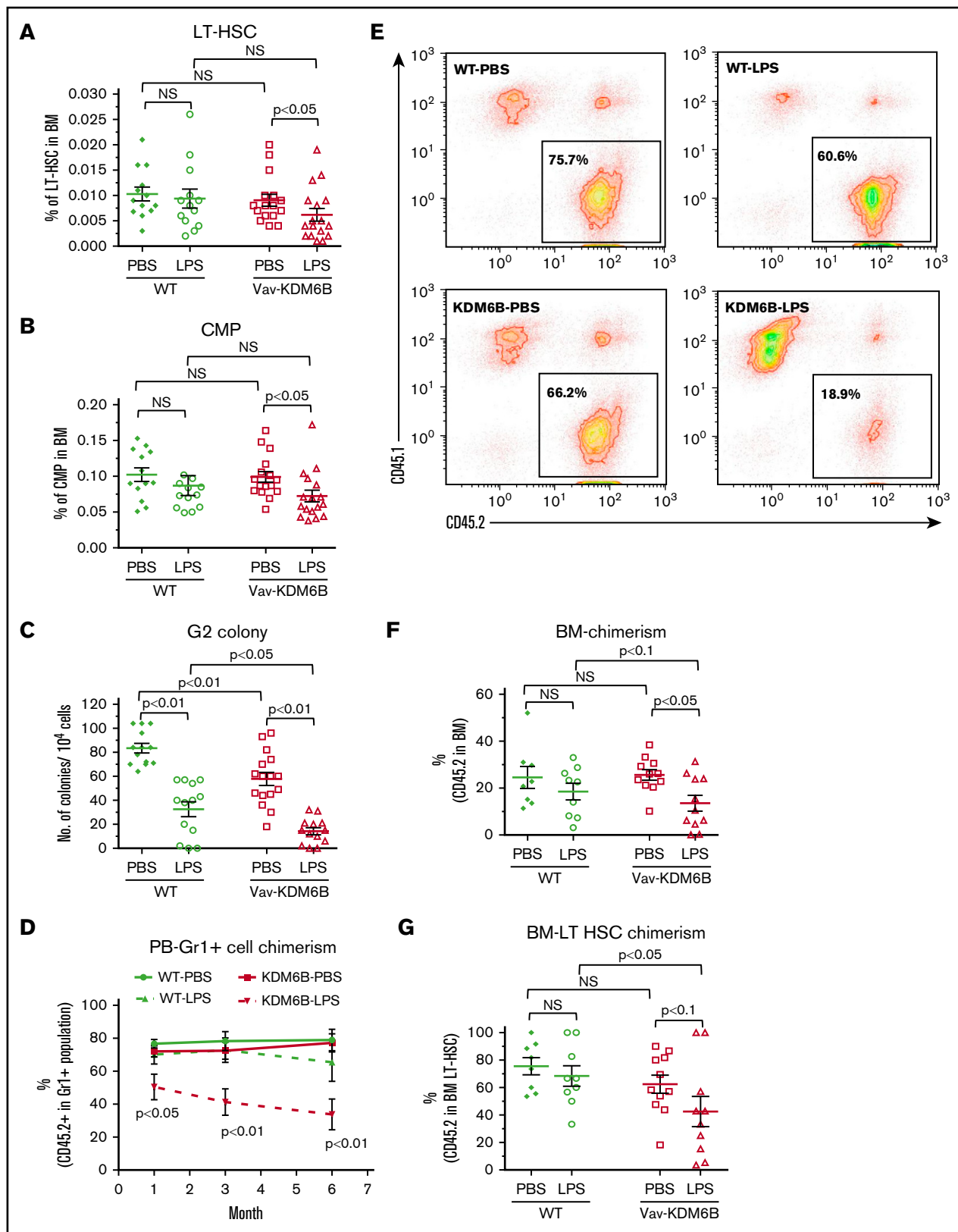


Figure 3. KDM6B overexpression combined with chronic low-dose LPS stimulation led to changes in BM hematopoietic stem and progenitor cells of mice. Results are based on adult Vav-KDM6B mice and wild-type (WT) controls treated with low-dose LPS (6 μ g/mouse) or PBS every other day for 6 weeks (LPS: N = 12 Vav-KDM6B, N = 13 WT; PBS: N = 16 Vav-KDM6B, N = 16 WT, unless otherwise noted). All error bars are based on \pm SEM. (A-B) Percentage of BM long-term hematopoietic

Next, we evaluated the pathophysiological relevance of KDM6B overexpression-mediated transcription activation by surveying a human CMML whole-exome RNA-Seq library (BM CD34⁺ HSPCs of 20 patients with CMML and 10 healthy control patients).²⁸ For 14 human homologs of murine genes upregulated in Vav-KDM6B LSKs, 10 are overexpressed in CMML (supplemental Figure 6B; $P < .0001$ for overlap) and 7 show a positive correlation with KDM6B (3 with $P < .05$), suggesting transcriptional activation mediated by KDM6B overexpression is involved in human disease.

We performed similar overlap analysis of the 135 genes identified in the LSKs of LPS-treated Vav-KDM6B mice. More than 30% ($N = 41$) are overexpressed in CMML (Figure 4C; $P < .05$ for overlap). This RNA signature has a statistically significant positive correlation of 0.50 with KDM6B mRNA level in CMML ($P = .028$). Gene set enrichment analysis indicated that these 135 genes were significantly associated with molecular signals relevant for MDS/CMML, especially innate immune pathways such as inflammatory, complement, and MAPK signaling (Figure 4B). They also significantly overlapped with the gene activation signature when *RPS14* was knocked down in human CD34⁺ BM cells, whereas *RPS14* is a gene with frequent heterozygous deletion in MDS/CMML (Figure 4B).

KDM6B overexpression mediates transcription activation via regulation of chromatin histone methylation

We previously reported that KDM6B overexpression in MDS BM HSPCs was associated with aberrant histone methylation at the promoters of innate immune genes.²¹ Therefore, we investigated whether transcriptional activation led by KDM6B overexpression in Vav-KDM6B mice was mediated by the regulation of histone methylation. *S100A9* is 1 of the genes upregulated in donor-derived Vav-KDM6B BM LSKs (supplemental Figure 6A) and encodes an important disease-driving innate immune activator in MDS.^{12,21} Compared with WT, both mRNA and promoter H3K4me3 of *S100a9* were significantly upregulated in Vav-KDM6B BM cells (Figures 5A-B). Alteration of promoter H3K27me3 was not detected for *S100a9* (data not shown).

Next we investigated the regulation of promoter histone methylation of *TLR1* and *C3*, 2 innate immune genes differentially activated by LPS treatment in Vav-KDM6B mice. In cultured BM cells, mRNA expression of *TLR1* and *C3* was elevated in LPS-treated Vav-KDM6B BM cells (Figures 5C-D). Compared with WT cells, promoter H3K4me3 of *TLR1* and *C3* was increased in Vav-KDM6B BM cells (Figures 5E-F). However, no further increase in H3K4me3 was detected when Vav-KDM6B BM cells were treated with LPS (Figure 5E-F). Similarly, nonsignificantly reduced H3K27me3 at these 2 genes was detected in BM cells from Vav-KDM6B mice compared with those from WT mice, but the reduction could

not be further enhanced by treatment with LPS (supplemental Figure 7A-B).

These data suggest that KDM6B overexpression alone results in epigenetic activation at the promoters of these innate immune genes, leading to limited but disease-relevant transcriptional activation. More profound overexpression of innate immune genes is a result of the cooperation between KDM6B-mediated histone modification and extra innate immune stimulation.

Pharmacologic targeting of KDM6B in murine and human MDS BM HSPCs could ameliorate compromised hematopoiesis

We next investigated whether pharmacologic inhibition of KDM6B could dampen innate immune signals and ameliorate the ineffective hematopoietic function of BM HSPCs in Vav-KDM6B mice. First, low doses (0.5 μ M) of GSK-J4,²⁹ a KDM6B-specific inhibitor, slightly decreased the expression of *S100a9* in Vav-KDM6B BM cells (supplemental Figure 8A) and also slightly inhibited the expression of *TLR1* and *C3* in LPS-treated Vav-KDM6B BM cells (supplemental Figure 8B-C). We then evaluated the effect of GSK-J4 on the BM repopulating capability of Vav-KDM6B mice. In LSKs from older Vav-KDM6B mice, GSK-J4 (0.5 μ M) significantly increased the number of colonies formed in second plating (G2; Figure 6A). In younger mice, GSK-J4 significantly increased the number of G2 colonies formed by LSKs of PBS- or LPS-treated Vav-KDM6B mice (Figure 6B) without affecting WT LSKs (Figure 6B).

We next assessed whether GSK-J4 could ameliorate the KDM6B overexpression-mediated impairment of BM HSPCs in vivo. We coinjected mice with GSK-J4 (8 mg/kg, 4 weeks) and LPS or PBS. Posttreatment, there was a tendency of slightly increased PB white blood cells (WBCs; supplemental Figure 9) and a significant increase of total BM cell counts (Figure 6C) in LPS-KDM6B mice that were coinjected with GSK-J4 compared with LPS-KDM6B without coinjection of GSK-J4. In subsequent competitive BM transplantation assays, CD45.2 BM cells were isolated from treated mice, mixed with CD45.1 WT competitive BM cells, and transplanted into lethally irradiated CD45.1 recipients. Coinjection of GSK-J4 with LPS in primitive Vav-KDM6B mice resulted in slightly increased PB CD45.2 chimerism compared with mice transplanted with BM cells of Vav-KDM6B mice treated by LPS only (Figure 6D).

Compromised BM HSPC repopulating capability is an important characteristic of MDS and CMML. Therefore we evaluated the effect of GSK-J4 on the repopulating capacity of primary MDS BM HSPCs. GSK-J4 (0.5 μ M) significantly increased colony formation in the BM CD34⁺ cells isolated from 14 untreated patients with MDS as compared with vehicle-treated cells (Figure 6E). GSK-J4 led to decreased AnnexinV ($P < .05$) and slightly increased CD71

Figure 3. (continued) stem cells (LT-HSCs) and common myeloid progenitors (CMP) in indicated mice. (C) G2 colony-forming units in serial methylcellulose colony formation assays using LSK BM cells isolated from donor mice (LPS: $N = 13$ Vav-KDM6B, $N = 13$ WT; PBS: $N = 17$ Vav-KDM6B, $N = 17$ WT). (D) Kinetics of peripheral blood myeloid (Gr1-positive) cell chimerism based on CD45.2 percentage in recipient mice (LPS: $N = 8$ Vav-KDM6B, $N = 9$ WT; PBS: $N = 11$ Vav-KDM6B, $N = 12$ WT). (E) Representative flow cytometry plots for CD45.2 cells from the peripheral blood of recipient mice 3 months after competitive transplantation by donor BM cells. (F-G) Cell chimerism in BM total cell and LT-HSC populations based on CD45.2 percentage in recipient mice 6 months after competitive transplantation (LPS: $N = 8$ Vav-KDM6B, $N = 9$ WT; PBS: $N = 11$ Vav-KDM6B, $N = 12$ WT)

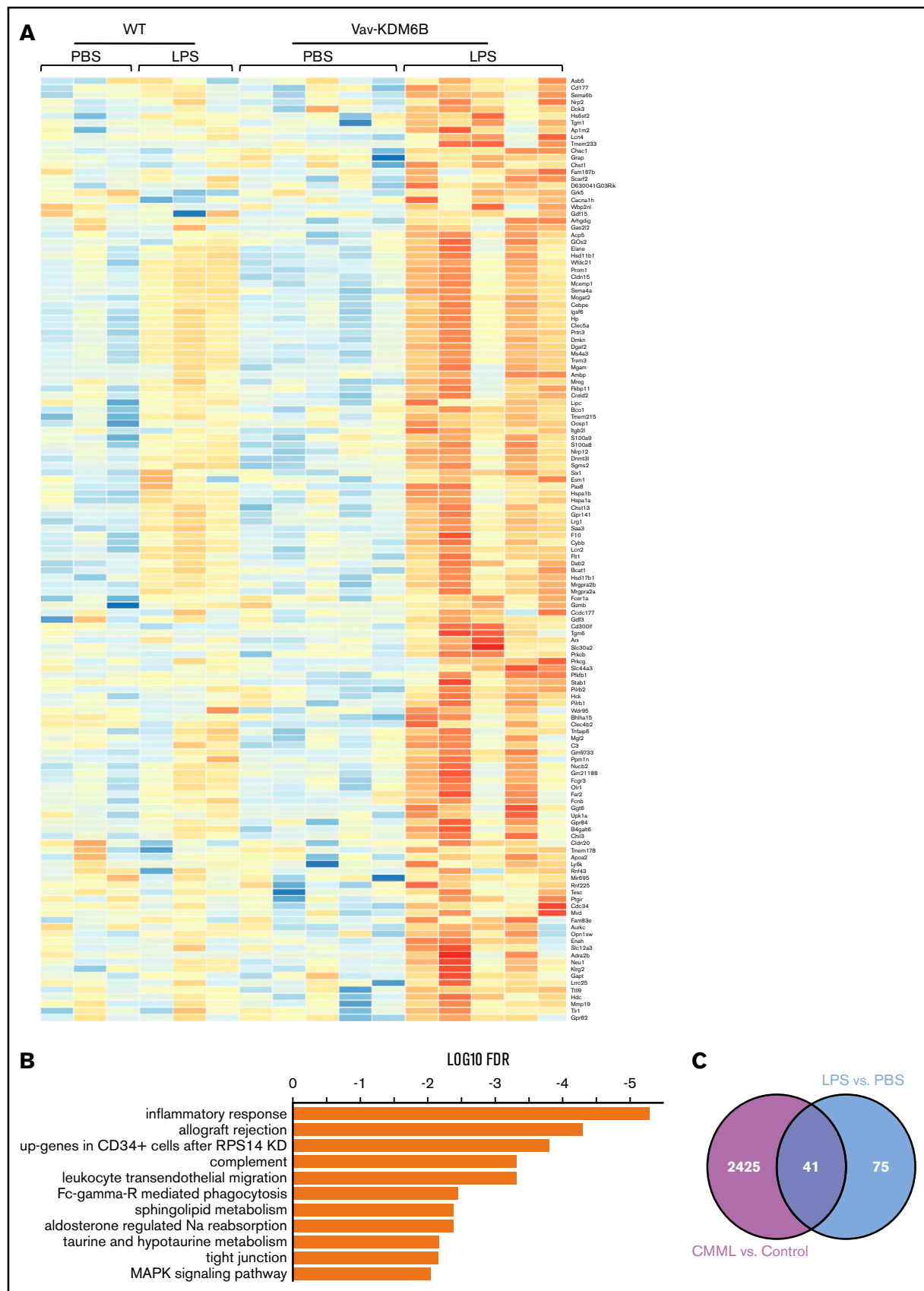


Figure 4.

($P < .1$) and CD11b ($P = .1$; supplemental Figure 10A-C). In these 14 cases, GSK-J4 led to a more than 2-fold increase of colony formation in 4 samples and 30% to 90% increase in 6 samples, and 4 samples had no response. Analysis of mRNA expression in available samples indicated that responding cases had a slight tendency ($P < .1$) toward higher KDM6B overexpression than nonresponders (supplemental Figure 10D). We tested the same dose of GSK-J4 in normal BM CD34⁺ cells from healthy donors (N = 4) and did not observe obvious differences in colony formation (supplemental Figure 10E).

Discussion

KDM6B is overexpressed in MDS and CMML and associated with dysregulation of innate immune genes.²¹ However, in relation to various limitations, the role of KDM6B overexpression in these heterogeneous myeloid disorders remains obscure. In the hematopoietic compartment, transcription of KDM6B can be activated by innate immune signals via NF- κ B.² Therefore, a critical question remains to be elucidated: Is overexpression of KDM6B a driving molecular aberration or just a bystander alteration resulting from the pro-inflammatory BM microenvironment in MDS and CMML? This question not only is important to better understand MDS/CMML pathophysiology but also is critical for developing targeted therapies. To provide a clear answer, we developed a novel mouse model that mimics the KDM6B overexpression of human MDS and CMML. Studies in this animal model demonstrated that KDM6B overexpression led to impairment of BM HSPCs and consequent ineffective hematopoiesis, thus providing direct evidence to support KDM6B overexpression as a molecular aberration contributing to MDS and CMML pathogenesis.

Vav-KDM6B mice have an age-dependent phenotype and shorter survival. Moreover, under chronic innate immune stimulation with LPS, Vav-KDM6B mice exhibited profound hematopoietic defects mimicking critical features of human MDS/CMML, including leukopenia, compromised repopulating capacity of BM HSPCs, and megakaryocytic dysplasia. Transcriptome studies revealed that KDM6B overexpression contributed to pathogenesis by driving activation of critical pathogenic genes such as *S100a9* with aging.^{12,21} Under inflammatory stress, KDM6B overexpression drove activation of more genes in the signal pathways driving MDS/CMML pathogenesis, including inflammatory, complement, and MAPK signaling. Finally, a KDM6B inhibitor (GSK-J4) ameliorated HSPC defects in both Vav-KDM6B mice and human patient samples. These results, together with our previous findings in patients,²¹ indicate that overexpression of KDM6B directly contributes to the pathogenesis of MDS/CMML, and that targeting KDM6B overexpression has therapeutic potential.

Consistent with previous studies, we observed that chronic inflammation, experimentally mimicked by low-dose LPS injection, led to mild hematopoietic consequences in WT mice.²⁶ In parallel, we observed that Vav-KDM6B mice in the absence of LPS exhibited

relatively mild hematopoietic alterations. Together, these results suggest that neither chronic inflammation nor KDM6B overexpression is sufficient to promote MDS/CMML pathogenesis. In contrast, the cooperation between KDM6B overexpression and chronic innate immune activation promotes an MDS/CMML-like phenotype. The effect of this cooperation in BM HSPCs was cell-intrinsic and was obvious in both in vitro and in vivo repopulating analyses. A study of KDM6B knockout mice indicated that the functional effect of KDM6B loss in murine myeloid cells could be detected only when the animals were under innate immune stimulation,³⁰ also suggesting that the function of KDM6B during hematopoietic differentiation was to mediate innate immune signals.

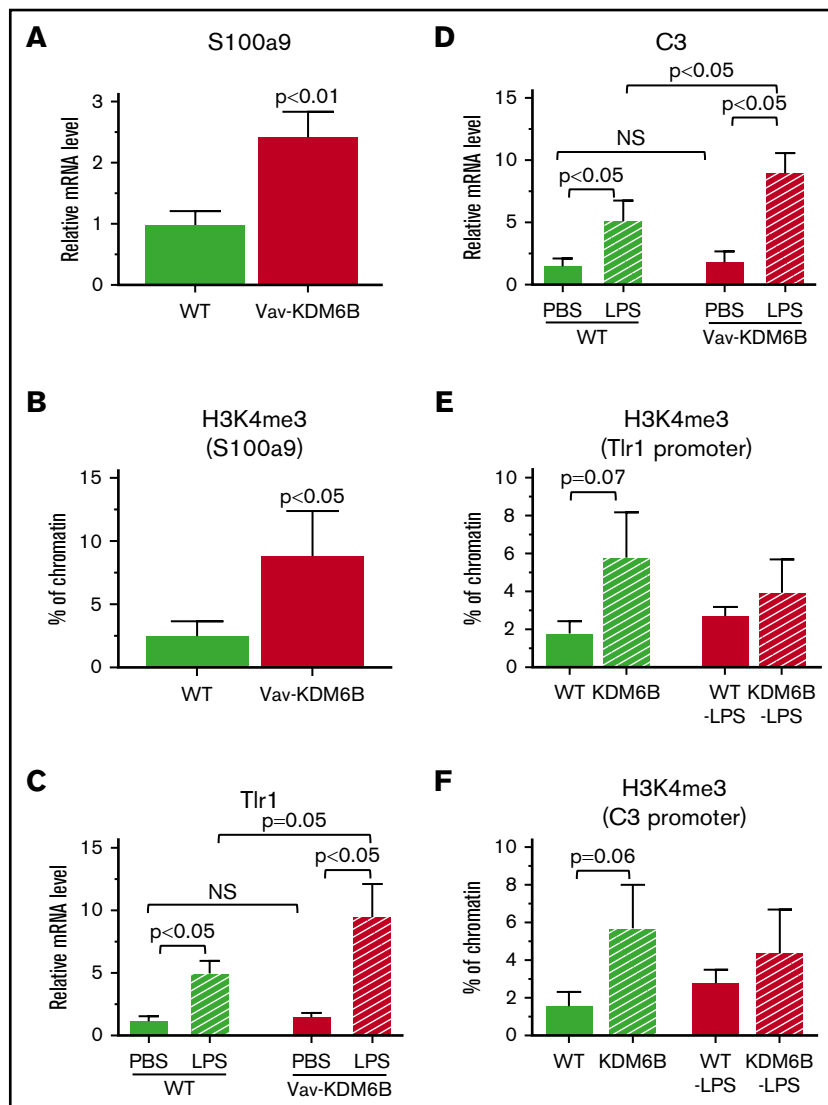
The concept of cooperation between chronic innate activation and KDM6B overexpression during pathogenesis was further confirmed by molecular profiling of mouse BM HSPCs. Consistent with the mild hematopoietic alterations in Vav-KDM6B mice that were not treated with LPS, RNA-Seq analysis indicated that KDM6B overexpression itself resulted in only limited transcriptional alterations in BM LSKs. However, although the number of genes hyperactivated by KDM6B overexpression alone was limited, overexpression of these genes is involved in MDS/CMML. More important, for the first time, we demonstrated that the *S100a9* gene, a key innate immune activator and disease-driving molecule during MDS pathogenesis, can be activated by KDM6B overexpression. The KDM6B gene is a transcriptional target of inflammatory and innate immune signals, and when activated, KDM6B forms a positive signal to further promote transcription of innate immune genes.

The RNA signature in BM HSPCs of Vav-KDM6B mice treated with LPS was associated with profound activation of innate immune and MDS-relevant genes. In addition, a subset of genes activated in BM HSPCs of LPS-treated Vav-KDM6B mice highly overlapped with genes known to be overexpressed in RPS14 knockdown human CD34⁺ BM HSPCs. RPS14 is a 5q-MDS haploinsufficient gene. Loss of RPS14 in mice has led to an MDS/CMML-like phenotype and activation of innate immune genes such as *S100A8/A9*.¹⁵ These results further indicate that disease-relevant lesions cross talk with KDM6B overexpression.

Analysis of histone methylation suggested that activation of key innate immune genes in Vav-KDM6B mice was mediated by KDM6B-regulated epigenetic modulation. At the regulatory regions of innate immune genes *S100a9*, *TLR1*, and *C3*, KDM6B overexpression increased the transcription-activating H3K4me3. These results suggest that KDM6B overexpression in the hematopoietic compartment can prime innate immune genes to an epigenetically open status that is sensitive to additional transcriptional stimulation, such as signals downstream of chronic innate immune activation. These results indicate that normal KDM6B expression is critical for restricting the functional effect of chronic inflammation in BM HSPCs. Consistent with

Figure 4. Chronic low-dose stimulation of Vav-KDM6B mice led to gene overexpression in BM LSK cells. (A) Heat map of the differentially activated genes in LSK BM cells of LPS-treated Vav-KDM6B mice. (B) Molecular pathways associated with the differentially activated genes in LSK BM cells of LPS-treated Vav-KDM6B mice, as revealed by gene set enrichment analysis. (C) Forty-one of the differentially activated genes in LSK BM cells of LPS-treated Vav-KDM6B mice were overexpressed in CD34-positive BM cells from patients with CMML (N = 20) compared with CD34-positive BM cells of healthy donors (N = 10). Results are based on RNA-Seq in mouse cells and RNA-Seq in human cells.

Figure 5. Overexpression of KDM6B in BM cells led to epigenetic activation of innate immune genes. (A) Quantitative reverse transcription reverse transcription-PCR results showing mRNA expression of the *S100a9* gene in mouse BM cells (N = 10 Vav-KDM6B, N = 13 WT). (B) Chromatin immunoprecipitation-PCR results showing H3K4me3 at the regulatory region of the *S100a9* gene in mouse BM cells (N = 5 in each group). (C-D) Quantitative reverse transcription-PCR results showing mRNA expression of innate immune genes *TLR1* and *C3* in mouse BM cells (treatment with LPS: N = 10 Vav-KDM6B, N = 8 WT; treatment with PBS: N = 12 Vav-KDM6B, N = 13 WT). (E-F) Chromatin immunoprecipitation-PCR results showing promoter H3K4me3 at the regulatory regions of the *TLR1* and *C3* genes (N = 5 in each group). All error bars are based on \pm SEM.



prior studies,^{27,30,31} we did not detect alteration of H3K27me3 at KDM6B-regulated genes, including *S100A9* in Vav-KDM6B cells. The mechanism of how KDM6B regulates innate immune genes should be further studied. Nevertheless, the identification of activation of *S100A9* and other innate immune genes further supports the role of KDM6B overexpression to enhance innate immune signals in BM HSPCs.

Most genetic lesions identified in MDS and CMML are associated with loss of biological function, indicating that targeted pharmacologic interference will be challenging.³ In contrast, targeting abnormal overexpression and gain of function of genes such as *KDM6B* may be feasible. Here, we provided initial evidence that the hematopoietic impairment associated with KDM6B overexpression, especially the compromised repopulating capability of BM HSPCs, can be ameliorated through pharmacologic inhibition of KDM6B. Using the KDM6B-specific inhibitor GSK-J4, hematopoiesis in both LPS-treated Vav-KDM6B mice and human MDS CD34⁺ cells was improved. Although GSK-J4 may affect both KDM6A and KDM6B, prior reports indicate that the anticancer and

anti-inflammation effects of GSK-J4 are closely related to interference of KDM6B.^{32,33} GSK-J4 did not affect hematopoiesis of WT mice or human BM HSPCs from healthy donors in our study. This result echoes our previous results of KDM6B knockdown in MDS CD34⁺ BM cells.¹¹ The dose of GSK-J4 that improved hematopoiesis in both mouse and human cells in this study was much lower, and it did not affect hematopoietic repopulation of normal BM HSPCs. There are several questions regarding KDM6B inhibition that should be addressed in future work, including characterization of GSK-J4 in transplanted mice and in other representative MDS/CMML models. Despite limitations, pharmacologic inhibition of KDM6B reported here was the first preclinical therapeutic study of GSK-J4 in MDS and CMML. Our group has recently reported the promising effect of targeting the innate immune activator TLR2 in patients with MDS (unpublished), and KDM6B shares common innate immune signaling pathways with TLR2. The preclinical effects reported here suggest that clinical trials assessing KDM6B inhibition in MDS should be developed.

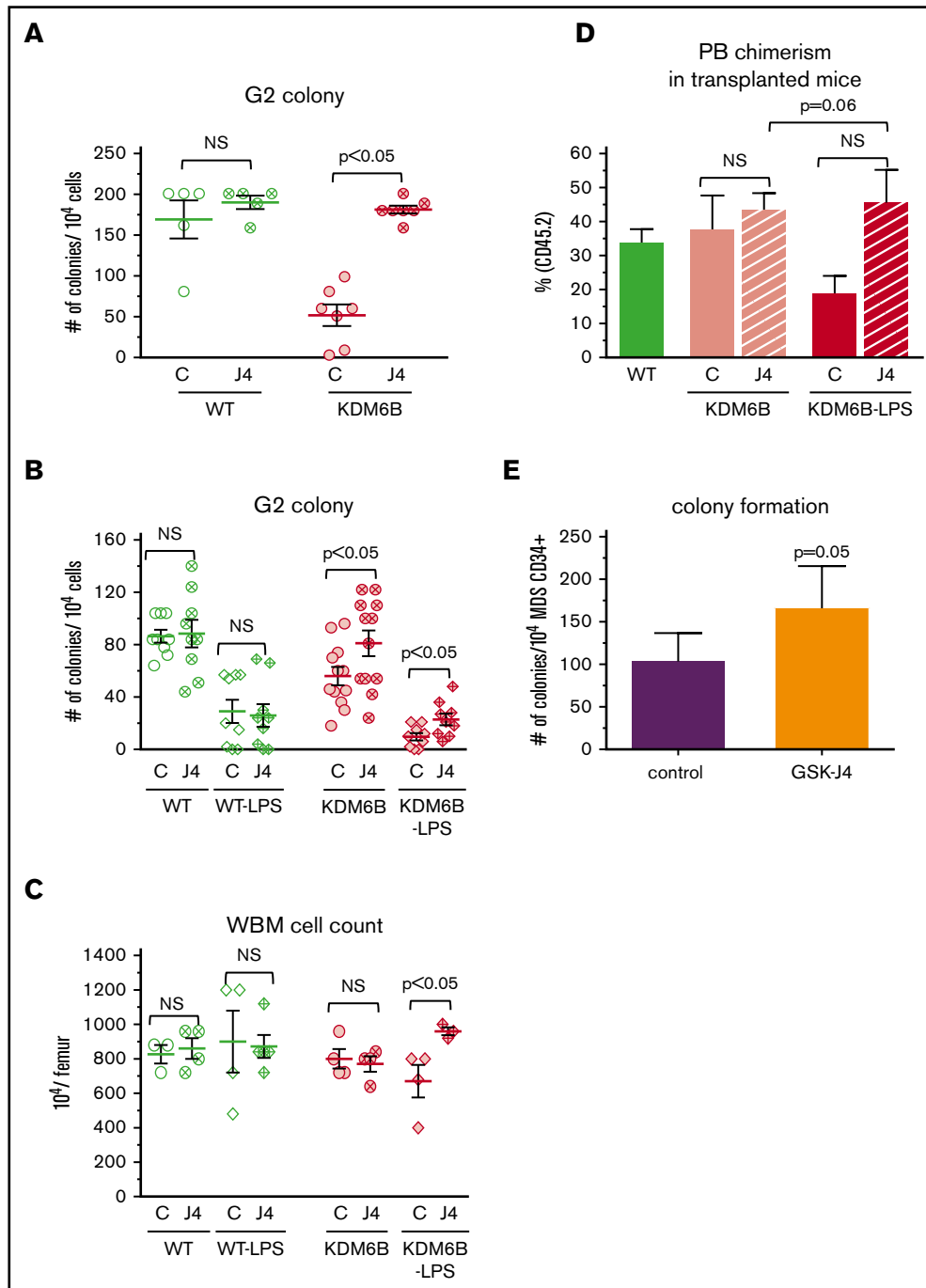


Figure 6. The KDM6B inhibitor GSK-J4 in mouse and human samples improved hematopoiesis. (A) Effect of GSK-J4 (0.5 μ M) on bone marrow (BM) repopulation capacity, based on G2 colony-forming units in serial methylcellulose colony formation assays using BM LSKs isolated from old, age-matched mice (aged >70 weeks; WT mice: N = 5 treated with control, N = 5 treated with GSK-J4; Vav-KDM6B mice: N = 7 treated with control, N = 7 treated with GSK-J4). (B) Effect of GSK-J4 (0.5 μ M) treated and LPS on BM repopulation capacity, based on G2 colony-forming units in serial methylcellulose colony formation assays using LSK BM cells isolated from old, age-matched mice (WT mice: N = 9 control, N = 8 GSK-J4 only, N = 9 LPS only, N = 9 LPS plus GSK-J4; Vav-KDM6B mice: N = 13 control, N = 13 GSK-J4 only, N = 10 LPS only, N = 10 LPS plus GSK-J4). (C-D) Effects of GSK-J4 (160 μ g/week for 4 weeks) on whole BM cell counts of WT mice and on PB chimerism in recipient mice (WT mice: N = 3 control, 4 GSK-J4 only, N = 4 LPS only, N = 5 LPS plus GSK-J4; Vav-KDM6B mice: N = 4 control, N = 4 GSK-J4 only, N = 4 LPS only, N = 3 LPS plus GSK-J4). (E) Effect of GSK-J4 (0.5 μ M) on hematopoiesis in low-risk MDS, based on colony-forming units in methylcellulose colony formation assays using primary MDS BM CD34-positive cells isolated from patients with untreated low-risk MDS (N = 11). All error bars are based on \pm SEM.

MDS and CMML are heterogeneous myeloid disorders, and numerous pathologic components drive their initiation and progression. We previously proposed that the overexpression of KDM6B cooperated with other molecular and cellular lesions to lead to MDS/CMML pathogenesis.²¹ In addition to cooperating with innate immune stimulation, it is important to determine whether KDM6B overexpression cooperates with other molecular lesions, such as common somatic mutations, to drive the development and progress of disease.

Acknowledgments

The authors thank Erica A. Goodoff from the Department of Scientific Publications and Kelly A. Soltysiak from the Department of Leukemia of ACC for editing the manuscript.

This study used the Research Histopathology Facility, Research Animal Support Resource, and Flow Cytometry & Cellular Imaging Facility, supported in part by the National Institutes of Health through MD Anderson Cancer Center (MDACC) Grant CA016672. Sequencing and analysis in this study used MDACC Science Park Next-Generation Sequencing Core supported by Cancer Prevention & Research Institute of Texas Award RP120348 and RP170002. This study was supported by Cancer Prevention & Research Institute of Texas Grant RP140500 and the Acute Myeloid

Leukemia/Myelodysplastic Syndromes Moon Shot of The University of Texas MD Anderson Cancer Center Moon Shot Program.

Authorship

Contribution: Y.W. and G.G.-M. conceived and designed the study; Y.W. developed the methodology; Y.W., H.Z., N.B., and S.J. acquired data; C.E.B.-R. and J.K. provided pathological analysis; C.C., Y.L., K.L., and K.-A.D. performed biostatistics analysis; H.Y. and I.G.-G. provided patient samples; and Y.W., D.T.S., S.C., and G.G.-M. wrote, reviewed, and revised the manuscript.

Conflict-of-interest disclosure: The authors declare no competing financial interests.

ORCID profiles: C.E.B.-R., 0000-0003-0180-7124; J.K., 0000-0003-2621-3584; C.C., 0000-0003-3130-3613; I.G.-G., 0000-0001-8354-3139; K.-A.D., 0000-0001-8710-7131.

Correspondence: Yue Wei, Department of Leukemia, Unit 428, The University of Texas MD Anderson Cancer Center, 1515 Holcombe Blvd, Houston, TX 77030; e-mail: ywei@mdanderson.org; and Guillermo Garcia-Manero, Department of Leukemia, Unit 428, The University of Texas MD Anderson Cancer Center, 1515 Holcombe Blvd, Houston, TX 77030; e-mail: ggarciam@mdanderson.org.

References

- Garcia-Manero G. Myelodysplastic syndromes: 2014 update on diagnosis, risk-stratification, and management. *Am J Hematol*. 2014;89(1):97-108.
- De Santa F, Totaro MG, Prosperini E, Notarbartolo S, Testa G, Natoli G. The histone H3 lysine-27 demethylase Jmjd3 links inflammation to inhibition of polycomb-mediated gene silencing. *Cell*. 2007;130(6):1083-1094.
- Woods BA, Levine RL. The role of mutations in epigenetic regulators in myeloid malignancies. *Immunol Rev*. 2015;263(1):22-35.
- Gañán-Gómez I, Wei Y, Starczynowski DT, et al. Dereglulation of innate immune and inflammatory signaling in myelodysplastic syndromes. *Leukemia*. 2015;29(7):1458-1469.
- Cabrero M, Wei Y, Yang H, et al. Down-regulation of EZH2 expression in myelodysplastic syndromes. *Leuk Res*. 2016;44:1-7.
- Moran-Crusio K, Reavie L, Shih A, et al. Tet2 loss leads to increased hematopoietic stem cell self-renewal and myeloid transformation. *Cancer Cell*. 2011;20(1):11-24.
- Challen GA, Sun D, Jeong M, et al. Dnmt3a is essential for hematopoietic stem cell differentiation. *Nat Genet*. 2011;44(1):23-31.
- Mochizuki-Kashio M, Aoyama K, Sashida G, et al. Ezh2 loss in hematopoietic stem cells predisposes mice to develop heterogeneous malignancies in an Ezh1-dependent manner. *Blood*. 2015;126(10):1172-1183.
- Wei Y, Dimicoli S, Bueso-Ramos C, et al. Toll-like receptor alterations in myelodysplastic syndrome. *Leukemia*. 2013;27(9):1832-1840.
- Fang J, Bolanos LC, Choi K, et al. Ubiquitination of hnRNPA1 by TRAF6 links chronic innate immune signaling with myelodysplasia. *Nat Immunol*. 2017;18(2):236-245.
- Dimicoli S, Wei Y, Bueso-Ramos C, et al. Overexpression of the toll-like receptor (TLR) signaling adaptor MYD88, but lack of genetic mutation, in myelodysplastic syndromes. *PLoS One*. 2013;8(8):e71120.
- Chen X, Eksioglu EA, Zhou J, et al. Induction of myelodysplasia by myeloid-derived suppressor cells. *J Clin Invest*. 2013;123(11):4595-4611.
- Rhyasen GW, Bolanos L, Fang J, et al. Targeting IRAK1 as a therapeutic approach for myelodysplastic syndrome. *Cancer Cell*. 2013;24(1):90-104.
- Keerthivasan G, Mei Y, Zhao B, et al. Aberrant overexpression of CD14 on granulocytes sensitizes the innate immune response in mDia1 heterozygous del(5q) MDS. *Blood*. 2014;124(5):780-790.
- Boldin MP, Taganov KD, Rao DS, et al. miR-146a is a significant brake on autoimmunity, myeloproliferation, and cancer in mice. *J Exp Med*. 2011;208(6):1189-1201.
- Varney ME, Niederkorn M, Konno H, et al. Loss of Tifab, a del(5q) MDS gene, alters hematopoiesis through derepression of Toll-like receptor-TRAF6 signaling. *J Exp Med*. 2015;212(11):1967-1985.
- Schneider RK, Schenone M, Ferreira MV, et al. Rps14 haploinsufficiency causes a block in erythroid differentiation mediated by S100A8 and S100A9. *Nat Med*. 2016;22(3):288-297.
- Starczynowski DT, Kuchenbauer F, Argiropoulos B, et al. Identification of miR-145 and miR-146a as mediators of the 5q- syndrome phenotype. *Nat Med*. 2010;16(1):49-58.

19. Jepsen K, Solum D, Zhou T, et al. SMRT-mediated repression of an H3K27 demethylase in progression from neural stem cell to neuron. *Nature*. 2007; 450(7168):415-419.
20. Sen GL, Webster DE, Barragan DI, Chang HY, Khavari PA. Control of differentiation in a self-renewing mammalian tissue by the histone demethylase JMJD3. *Genes Dev*. 2008;22(14):1865-1870.
21. Wei Y, Chen R, Dimicoli S, et al. Global H3K4me3 genome mapping reveals alterations of innate immunity signaling and overexpression of JMJD3 in human myelodysplastic syndrome CD34+ cells. *Leukemia*. 2013;27(11):2177-2186.
22. Robinson MD, McCarthy DJ, Smyth GK. edgeR: a Bioconductor package for differential expression analysis of digital gene expression data. *Bioinformatics*. 2010;26(1):139-140.
23. Ogilvy S, Elefanty AG, Visvader J, Bath ML, Harris AW, Adams JM. Transcriptional regulation of vav, a gene expressed throughout the hematopoietic compartment. *Blood*. 1998;91(2):419-430.
24. Ogilvy S, Metcalf D, Gibson L, Bath ML, Harris AW, Adams JM. Promoter elements of vav drive transgene expression in vivo throughout the hematopoietic compartment. *Blood*. 1999;94(6):1855-1863.
25. Perrigue PM, Silva ME, Warden CD, et al. The histone demethylase jumonji coordinates cellular senescence including secretion of neural stem cell-attracting cytokines. *Mol Cancer Res*. 2015;13(4):636-650.
26. Esplin BL, Shimazu T, Welner RS, et al. Chronic exposure to a TLR ligand injures hematopoietic stem cells. *J Immunol*. 2011;186(9):5367-5375.
27. Zhao W, Li Q, Ayers S, et al. Jmjd3 inhibits reprogramming by upregulating expression of INK4a/Arf and targeting PHF20 for ubiquitination. *Cell*. 2013; 152(5):1037-1050.
28. Colla S, Ong DS, Ogoti Y, et al. Telomere dysfunction drives aberrant hematopoietic differentiation and myelodysplastic syndrome. *Cancer Cell*. 2015; 27(5):644-657.
29. Kruidenier L, Chung CW, Cheng Z, et al. A selective jumonji H3K27 demethylase inhibitor modulates the proinflammatory macrophage response. *Nature*. 2012;488(7411):404-408.
30. Satoh T, Takeuchi O, Vandenbon A, et al. The Jmjd3-Irf4 axis regulates M2 macrophage polarization and host responses against helminth infection. *Nat Immunol*. 2010;11(10):936-944.
31. De Santa F, Narang V, Yap ZH, et al. Jmjd3 contributes to the control of gene expression in LPS-activated macrophages. *EMBO J*. 2009;28(21): 3341-3352.
32. Hashizume R, Andor N, Ihara Y, et al. Pharmacologic inhibition of histone demethylation as a therapy for pediatric brainstem glioma. *Nat Med*. 2014; 20(12):1394-1396.
33. Ntziachristos P, Tsigos A, Welstead GG, et al. Contrasting roles of histone 3 lysine 27 demethylases in acute lymphoblastic leukaemia. *Nature*. 2014; 514(7523):513-517.